Atmos. Chem. Phys., 10, 8205–8218, 2010
www.atmos-chem-phys.net/10/8205/2010/
doi:10.5194/acp-10-8205-2010

Atmospheric Chemistry and Physics

The effects of clouds and aerosols on net ecosystem CO_2 exchange over semi-arid Loess Plateau of Northwest China

X. Jing[1], J. Huang[1], G. Wang[1], K. Higuchi[2], J. Bi[1], Y. Sun[1], H. Yu[1], and T. Wang[1]

[1]Key Laboratory for Semi-Arid Climate Change of the Ministry of Education, College of Atmospheric Sciences, Lanzhou University, Lanzhou, 730000, China
[2]Adaptation and Impacts Division, Environment Canada, Toronto, Canada

Received: 5 March 2010 – Published in Atmos. Chem. Phys. Discuss.: 26 May 2010
Revised: 29 August 2010 – Accepted: 30 August 2010 – Published: 2 September 2010

Abstract. The impacts of clouds and atmospheric aerosols on the terrestrial carbon cycle at semi-arid Loess Plateau in Northwest China are investigated, by using the observation data obtained at the SACOL (Semi-Arid Climate and Environment Observatory of Lanzhou University) site. Daytime (solar elevation angles of larger than 50°) net ecosystem exchange (NEE) of CO_2 obtained during the midgrowing season (July–August) are analyzed with respect to variations in the diffuse radiation, cloud cover and aerosol optical depth (AOD). Results show a significant impact by clouds on the CO_2 uptake by the grassland (with smaller LAI values) located in a semi-arid region, quite different from areas covered by forests and crops. The light saturation levels in the canopy are low, with a value of about 434.8 $W\,m^{-2}$. Thus, under overcast conditions of optically thick clouds, the CO_2 uptake increases with increasing clearness index (the ratio of global solar radiation received at the Earth surface to the extraterrestrial irradiance at a plane parallel to the Earth surface), and a maximum CO_2 uptake and light use efficiency of vegetation occur with the clearness index of about 0.37 and lower air temperature. Under other sky conditions, CO_2 uptake decreases with cloudiness but light use efficiency is enhanced, due to increased diffuse fraction of PAR. Additionally, under cloudy conditions, changes in the NEE of CO_2 also result from the interactions of many environmental factors, especially the air temperature. In contrast to its response to changes in solar radiation, the carbon uptake shows a slightly negative response to increased AOD. The reason for the difference in the response of the semi-arid grassland from that of the forest and crop lands may be due to the difference in the canopy's architectural structure.

Correspondence to: J. Huang
(hjp@lzu.edu.cn)

1 Introduction

Solar radiation is a major factor that influences the CO_2 exchange in the biosphere. Several researchers have suggested that the diffuse radiation proportion in the solar radiation can result in higher light use efficiency than direct radiation (Goudriaan, 1977; Gu et al., 2002, 2003; Roderick et al., 2001). It is well known that changes in cloud cover or atmospheric aerosol loadings, arising from either volcanic or anthropogenic emissions, alter both the total solar radiation reaching the surface and the fraction of diffuse radiation, with uncertain overall effects on global plant productivity and the land carbon sink (Mercado et al., 2009). Additionally, the diffuse fraction of the solar radiance incident at the earth's surface has increased substantially in many regions as a consequence of increases in both cloudiness and the concentration of aerosols in the atmosphere (Suraqui et al., 1974; Abakumova et al., 1996). In forests, higher light use efficiencies and carbon uptake have been demonstrated by field observations for cloudy and high aerosols conditions (Price and Black, 1990; Hollinger et al., 1994; Fitzjarrald et al., 1995; Gu et al., 1999; Freedman et al., 1998, 2001; Niyogi et al., 2004).

Previous studies have focused mainly on the forest canopy, with larger leaf area index (LAI) and higher photosynthetic capacity. Under cloudy conditions and with aerosol loading, there is broad consensus on the impact of diffuse radiation on terrestrial ecosystem carbon cycle (Fitzjarrald et al., 1995; Gu et al., 1999; Roderick et al., 2001; Niyogi et al., 2004; Oliveira et al., 2007), especially for the North American forests. However, the relationship between clouds and ecosystem CO_2 exchange can be more complicated, due to changes in other environmental factors that could influence the ecosystem carbon cycle. For example, changes in vapor pressure deficit (VPD), air and soil temperature (Freedman et

al., 1998; Gu et al., 1999, 2002) can have significant impact on the carbon exchange processes. Although there have been numerous studies about the effect of diffuse radiation caused by clouds and aerosols on the ecosystem carbon cycle, few have investigated the case over semi-arid region with short-stature canopies. Due to smaller LAI values and weaker photosynthesis capacities for short canopies, the positive effect of diffuse radiation may be reduced or non- existent (Letts et al., 2005). Until now, there have been only a few observations on the CO_2 flux and boundary layer meteorological conditions over the semi-arid Loess Plateau of Northwest China.

Arid and semi-arid areas comprise about 30% of the Earth's land surface. Climate change and climate variability will likely have a significant impact on these regions. The faster warming of semi-arid Loess Plateau region under global warming (Yao et al., 2005a, b) has resulted in rapid degradation of fragile vegetative ecological resources in these regions (Liu et al., 2006). The cloud cover has reduced but the cloud optical depth has risen in the 15 years over Northwestern China (Chen et al., 2005). With natural and anthropogenic activities, combined with sparse vegetation, fragile ecosystems, and little precipitation that shows a decreasing trend in recent years (Song and Zhang, 2003), the semi-arid region of the Loess Plateau in Northwest China produces large amounts of dust and other types of aerosols. The variability of environmental factors may result in significant effects on regional climate, especially the radiative forcing, via the biogeochemical pathways affecting the terrestrial carbon cycle. Thus, in this study we attempt to answer the following questions: (1) what is the net ecosystem exchange (NEE) of CO_2 for the short-grass vegetation in the semi-arid Loess Plateau region? (2) How important is the influence of diffuse radiation on the carbon uptake in the region? (3) How will the NEE of CO_2 change with cloudiness? and (4) How does the aerosol loading affect the short grass NEE? With the ecosystems already adapted to the environment, the Loess Plateau region serves as an ideal location to investigate the impact of clouds and aerosols on the carbon uptake associated with semi-arid vegetation.

2 Site and measurement

2.1 Site description

The study site (35°57′ N, 104°08′ E), established in 2006, is the Semi-Arid Climate and Environment Observatory of Lanzhou University (SACOL), which is a long-term meteorological observatory operated by the College of Atmospheric Sciences, Lanzhou University. It is located at an elevation of 1965.8 m, about 48 km away from the centre of Lanzhou, Gansu province in northwestern China. The station is situated at the southern bank of Yellow River, a semi-arid area on the Loess Plateau in China, and is part of the temperate zone semi-arid area. The soil parent material is mainly quaternary aeolian loess with the soil type of Sierozem according to the Chinese Soil Classification System (Chinese Soil Taxonomy Cooperative Research Group, 1995). The terrain where the measurements are carried out is flat, mainly covered by short grass with species of *stipa bungeana*, *artemisia frigida* and *leymus secalinus*, which belong to C3. The site is located on a nearly north-south mesa with a fetch length of about 120 m in the most common wind direction. The mesa has a limited width of about 200 m from the east to the west, and is about 600 m in length from the north to the south. There is a large V-shaped valley to the west of the site and a small one to the east. Figure 1 shows the typical seasonal vegetation around the site. The short growing season, strong radiation and little precipitation result in sparse vegetation coverage, mainly short grass. During the 2007 growing season the height of grassland averaged 14.7 cm, with an averaged leaf area index (LAI) of 0.37. In this fragile ecosystem, the net atmosphere-biosphere CO_2 exchange will be less than that observed in forests and croplands, but the sensitivity of the semi-arid ecosystems to extreme environmental conditions that exist at the study site makes it useful for investigating ecosystem response (in terms of CO_2 flux) to changes in solar radiation induced by differing amounts of clouds and aerosols. More details relating to the site and instrumentation can be found in a report by Huang et al. (2008).

2.2 Measurements

At the SACOL site, the turbulent flux measurement system consists of a three-axis sonic anemometer (CSAT3, Campbell) to measure three wind components and sonic virtual temperature, and an open path infrared CO_2/H_2O analyzer (LI7500LI-COR) to measure $CO_2$and H_2O concentrations. The sensor for measuring CO_2 and H_2O turbulence (LI7500) are calibrated in May every year. The observations are taken at 2.88 m above the ground surface with signals acquired by a CR5000 (Campbell) data logger at 10 Hz. From the raw data, half-hourly fluxes are calculated. The ecosystem eddy carbon dioxide fluxes are measured using eddy covariance methods (Zuo et al., 2009). A slow response humidity and temperature probe (HMP45C-L, Vaisala) is also set near and at the same level of the open-path eddy covariance flux system. Supporting data include measurements of the surface skin temperature (IRTS-P, Apogee), soil temperature at depths of 2, 5, 10, 20, 50, and 80 cm (STP01-L, Hukseflux), and soil moisture at depths of 5, 10, 20, 40, and 80 cm (CS616-L, Campbell). Using a 32 m surface layer meteorological tower as a measurement platform, wind speed (014A-L, Met One), air temperature and vapor pressure (HMP45C-L, Vaisala) at 1, 2, 4, 8, 12, 16 and 32 m, and wind direction (034B-L, Met One) at 8 m are determined, with signals logged to a data logger (CR23X, Campbell) and recorded at half-hour intervals. In addition, at the

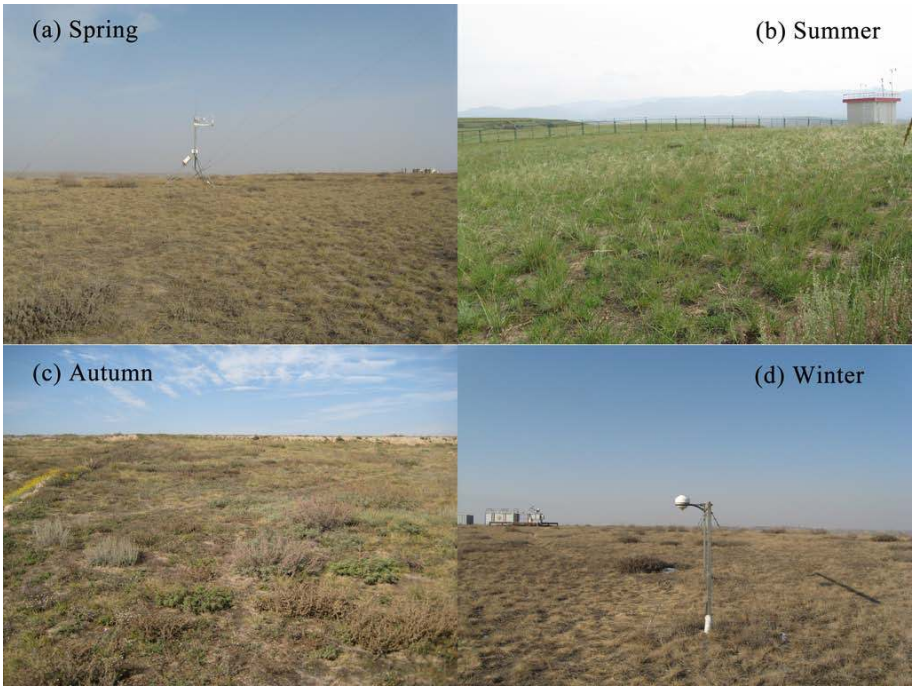

Fig. 1. Seasonal vegetation views of the SACOL site.

SACOL site there is a full surface radiation monitoring system equipped with pyranometers and sun trackers (CM21 and CG4, Kipp and Zonen) at a height of 1.5 m. The total solar radiation is measured directly with CM21 pyranometer which is fixed on the solar tracker (2AP, Kipp and Zonen), and the diffuse radiation is measured using CM21 pyranometer with a shade ring. The long-term turbulent exchange, as well as boundary layer meteorological and radiation measurements at the SACOL site provide a unique opportunity to investigate the effects of aerosols and clouds on the CO_2 uptake over an arid and semi-arid region.

The observations of aerosol optical depth (AOD) are made using an automatic sun tracking photometer (CE318N-VPS8, Cimel) (Holben et al., 1998) at the SACOL site, with 8 filters at the visible and near infrared wavelengths of 340, 380, 440, 500, 675, 870, 937, 1020 nm. In this study, we use the 500 nm data, which corresponds to a photosynthetically active radiation (PAR) wavelength (400–700 nm). The AOD measurements are available for cloud free conditions since they are screened for clouds by analyzing a sequence of three sets of measurements taken 30 s apart as described in Holben et al. (2001). In order to completely reject the effect of clouds, only the AOD data under clear sky conditions are analyzed. The AOD measurements are performed on an irregular time schedule, usually at periods less than half an hour; these are then interpolated linearly to half-hourly data. Periods with missing eddy CO_2 flux (F_e) or AOD measurements are not used in this study.

In order to minimize the effects of changing leaf area, day time, solar elevation angle and environmental factors, only the mid-growing season data from July to August in 2007 are selected (the period which includes the peak photosynthetic activity and capacity of the canopy). Since our study is focused on the effect of clouds and aerosols on the photosynthetic activity of the ecosystem around our site, we have selected for the analysis only those data obtained when the solar elevation angle is larger than 50°. The early morning and evening periods are eliminated to avoid confounding influence from low solar angles on the diffuse radiation fraction caused by the cloud cover or aerosol loading (Gu et al., 1999).

3 Methods

3.1 Calculation of net ecosystem CO_2 exchange

The net ecosystem CO_2 exchange (NEE) between the semi-arid grass ecosystem and the atmosphere consists of two components: a turbulent eddy flux transported across the plane of instrumentation above the grassland (F_e), and exchange below the instrumentation height, which is manifested as a change in the storage of CO_2 in the air column above the grass ($F_{\Delta S}$). The net flux of CO_2 crossing the plane at our instrumentation height is calculated as the mean covariance between fluctuations in the vertical wind velocity (w) and the density of CO_2 (c) (Baldocchi et al., 1988):

$$F_e = \rho(\overline{w'c'}) \quad (1)$$

where ρ is the density of air, the primes denote deviations from the mean and the overbar signifies a time average. We use the general convention of designating carbon flux out of the ecosystem as positive. The flux associated with a change in the storage ($F_{\Delta S}$) is calculated as:

$$F_{\Delta S} = \frac{\Delta c}{\Delta t} H \quad (2)$$

where $\frac{\Delta c}{\Delta t}$ is the change in CO_2 concentration per unit time, and H is the height of the instrumentation plane. For the short grass, due to the negligible concentration gradient of CO_2 inside the vegetation canopy, we use the half-hourly change in the concentration at 2.88m as Δc for our estimates of $F_{\Delta S}$. The NEE of CO_2 (F_c) between the ecosystem and the atmosphere is the sum of the eddy and the Δ-storage fluxes:

$$F_c = F_e + F_{\Delta S} \quad (3)$$

Furthermore, for the purpose of this study, we can put F_c as the difference between the ecosystem respiration rate (R_e) and the photosynthetic flux density (P):

$$F_c = R_e - P \quad (4)$$

Respiration from soil heterotrophs and plant maintenance is strongly influenced by temperature (Jarvis and Leverenz, 1983; Norman and Arkebauer, 1991). At the SACOL site, the nighttime NEE is relatively small and remains nearly steady with increasing temperature. We estimate the respiration during the daytime periods using the empirical function given by Gu et al. (2002):

$$R_e = c_1 e^{c_2[c_3 T_a + (1-c_3)T_s]} + d_1 e^{d_2 T_s} \quad (5)$$

where c_1, c_2, c_3, d_1, and d_2 are the regression coefficients, T_s is the soil temperature at the 5-cm depth, and T_a is the air temperature at the 2-m height. The first term on the right hand side of Eq. (5) is expected to capture the aboveground biomass respiration, while the second is expected to capture the soil respiration. We assume the nighttime NEE to be the total ecosystem respiration, and use the optimization procedure to get the regression coefficients. We then use Eq. (5) to calculate the daytime respiration rate. Finally, photosynthesis is calculated from the estimated respiration and NEE.

3.2 Clearness index

Solar radiation intensity is converted to a clearness index (CI), which can describe the sky conditions. It is defined as the ratio of global solar radiation received at the Earth surface to the extraterrestrial irradiance at a plane parallel to the Earth surface. It is calculated by

$$\mathrm{CI} = \frac{S}{S_e} \quad (6a)$$

$$S_e = S_{sc}[\,1.000109 + 0.033494\cos X + 0.001472\sin X + 0.000768\cos(2X) + 0.000079\sin(2X)\,]\sin\beta \quad (6b)$$

$$X = 2\pi\frac{t_d - 1}{365} \quad (6c)$$

where CI denotes the clearness index, S denotes the total irradiation received at the Earth surface ($\mathrm{W\,m^{-2}}$), S_e is the extraterrestrial irradiance at a plane parallel to the Earth surface ($\mathrm{W\,m^{-2}}$), S_{sc} is the solar constant ($1367\,\mathrm{W\,m^{-2}}$), β is the solar elevation angle calculated by using the algorithm given by Michalsky (1988), t_d denotes the day of year, and X is the angle in the day of year.

3.3 Total PAR and diffuse PAR

To identify the potential factors controlling and contributing to the influence of aerosols and clouds on the carbon uptake, we also study the relationships between NEE and the total PAR, diffuse PAR, VPD, air temperature, and soil temperature. At SACOL the total PAR and diffuse PAR are not measured. Therefore we calculate the total PAR using the equation for climatological estimation given by Zhou (1996):

$$\mathrm{PAR_t} = \eta u S \quad (7a)$$

$$\eta = a + b\lg E^* \quad (7b)$$

where PAR_t is the total PAR ($\mu\mathrm{mol\,photon\,m^{-2}\,s^{-1}}$), u=4.55 $\mu\mathrm{mol\,J^{-1}}$, is an average of conversion quantum coefficient given by Zhou et al. (1996), $E^* = \frac{P_0}{P}E$, P_0 and P are the standard atmospheric pressure and atmospheric pressure of measurement station, respectively, E is the surface vapor pressure (hPa), a=0.404 and b=0.051 are both empirical coefficients, which are acquired from the work by Ji et al. (1993) over the Zhangye region in the semi-arid Loess Plateau of Northwest China. The detailed explanations about the calculation of the total PAR can be found in Zhou et al. (1996) and Ji et al. (1993). To determine the diffuse component of the total PAR, Spitters et al. (1986) proposed the following relationship:

$$\mathrm{PAR_f} = \frac{[1 + 0.3(1-q^2)]q}{1 + (1-q^2)\cos^2(90^\circ - \beta)\cos^3\beta}\mathrm{PAR_t} \quad (8)$$

where $\mathrm{PAR_f}$ is the diffuse PAR ($\mu\mathrm{mol\,photon\,m^{-2}\,s^{-1}}$) and $q = (S_f/S_e)/\mathrm{CI}$, S_f denotes the total diffuse radiation received by a horizontal plane on the Earth surface ($\mathrm{W\,m^{-2}}$).

The fraction of the diffuse PAR (D_f) is defined as the ratio of diffuse PAR ($\mathrm{PAR_f}$) to the total PAR ($\mathrm{PAR_t}$). Additionally, in order to eliminate the effect of decreased solar radiation on the CO_2 flux (e.g., due to clouds), we normalize the NEE and $\mathrm{PAR_f}$ values by $\mathrm{PAR_t}$, used to express the light use efficiency (LUE) of vegetation and the fraction of diffuse PAR (D_f), respectively.

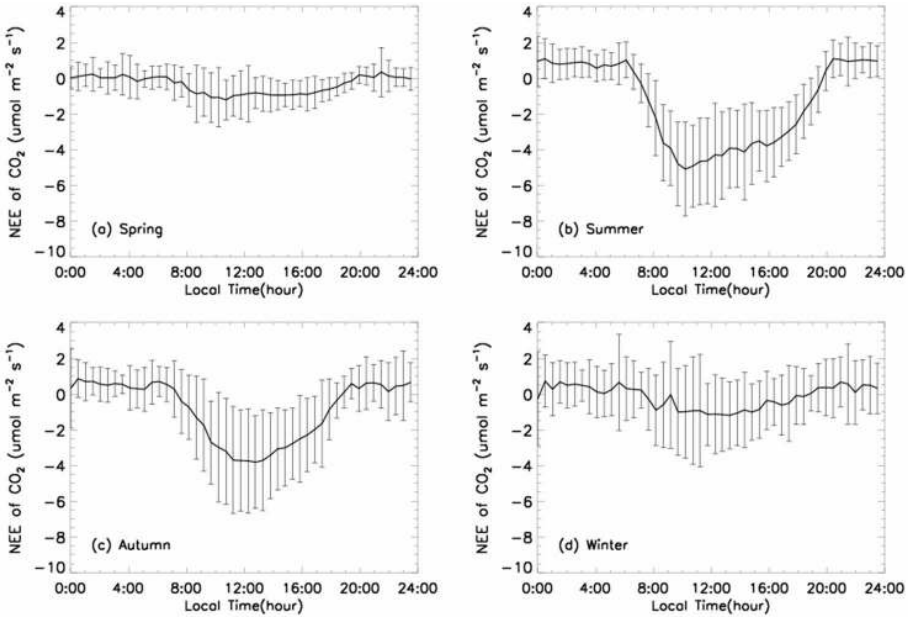

Fig. 2. Seasonally averaged diurnal cycles and associated standard deviation of NEE of CO_2 for 2007.

3.4 Cloudiness

Since no direct cloud observations are made at the SACOL site, we estimate the degree of cloudiness by using the method established by Long et al. (2000, 2006) and analyze the 1-min measurements of surface downward total and diffuse shortwave irradiance to identify periods of clear sky and estimate fractional sky cover. In order to ensure the precision of the method, we compare the result to the global irradiation time series plots, site logs and the Lidar data, and eliminate the data with significant errors. More details relating to the estimating of cloudiness can be found in Appendix A.

4 Results analysis

4.1 Diurnal cycle of NEE

Figure 2 shows the seasonally averaged diurnal cycle and standard deviation of the NEE (F_c, 30-min averages) in 2007 over the semi-arid Loess Plateau of Northwest China. In winter and spring, we note that the averaged daytime NEE is shown to be negative (i.e., the net CO_2 flux is into the vegetation). This is inconsistent with the fact that the ecosystem is dormant and frozen during this part of the year. The measurement errors may be caused by the instrument surface heat exchange affecting the open-path CO_2 flux measurements (Burba et al., 2008). In summer and autumn, the seasonally averaged carbon flux exceeds $-5.0\,\mu mol\,m^{-2}\,s^{-1}$ (in July and August, the monthly averaged NEE can reach around $-6.5\,\mu mol\,m^{-2}\,s^{-1}$, not shown), but the amount of carbon uptake is still much less than those observed in forests and croplands (Niyogi et al., 2004). It is also less than that observed in the semi-arid area in Tongyu (44°25′ N, 122°52′ E) and in the typical steppe prairie in Inner Mongolia (44°08′31″ N, 116°18′45″ E) both covered by grassland and can reach $-18\,\mu mol\,m^{-2}\,s^{-1}$ (Liu et al., 2006) and $-14\,\mu mol\,m^{-2}\,s^{-1}$ (Gao et al., 2009) in summer, respectively. During the summer (June–August), we observe significant diurnal variation in NEE, with a relatively steady respiration (net carbon output from the vegetation) and a strong photosynthesis that tracks the solar radiation during the daytime from 06:00 to 20:00 LT. However, the maximum carbon uptake takes place around 10:00 LT, rather than at midday. We also observe that the carbon flux during the daytime shows larger day-to-day fluctuations (larger standard deviation, Fig. 2) than the nighttime. This is likely due to variations in the various processes that influence the level of photosynthetic and respiration activity from day to day, with the possibility that diffuse radiation plays a significant role in affecting the photosynthesis. The effect of increased diffuse radiation fraction can be related to increased cloud cover and/or aerosol loading, which can alter the proportion of diffuse radiation in global solar radiation reaching the Earth's surface.

4.2 Effect of diffuse radiation

Clearness Index (CI) can describe the sky conditions and solar radiation intensity. Change in the surface NEE of CO_2 with CI is shown in Fig. 3 for the period from July to August of 2007. The CI value typically ranges from 0.05 to 0.85. Although the plotted values show a large scatter, a cubic regression curve fitted to the data delineates a relationship in which NEE reaches a minimum (maximum net uptake by the

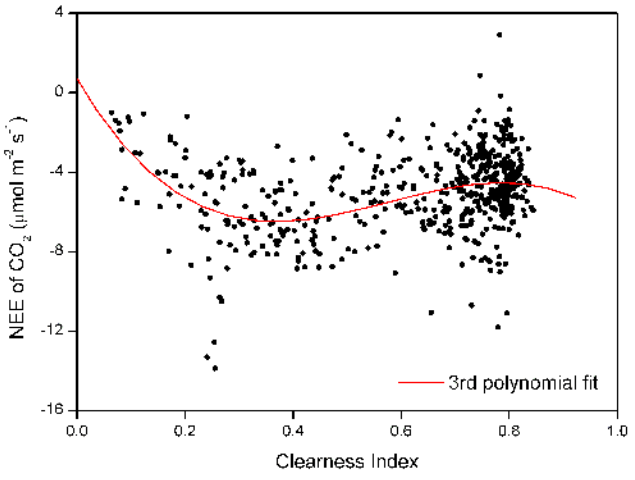

Fig. 3. Relationship of 3rd polynomial fit ($n = 540$, $r^2 = 0.15$, $p < 0.01$) between 30-min averaged NEE and clearness index.

vegetation) with a CI value of about 0.37 (corresponding to the solar radiation of about 434.8 W m^{-2}) for the short grass over semi-arid regions. The value is in the low end of the range 0.4–0.7 observed for some forest systems (Gu et al., 1999; Oliphant et al., 2002). It indicates that the vegetation at the observation site have a low light saturation.

It is well known that there is a significant benefit to ecosystem productivity from increased diffuse radiation because plant canopies use diffuse radiation more efficiently than they use direct beam radiation for photosynthesis (Goudriaan, 1977; Gu et al., 2002, 2003). Figure 4a–c show changes in the total PAR, diffuse PAR and fraction of diffuse PAR as a function of CI at the SACOL site, respectively. Although the total PAR increases almost linearly as CI increases (Fig. 4a), the relationship between the diffuse PAR and the CI is not linear (Fig. 4b), as with the relationship between the fraction of diffuse PAR and the CI (Fig. 4c). Although there is a large scatter in the data, diffuse PAR shows a general increase with increasing CI, reaching a maximum for CI in a range 0.5 to 0.6 (Fig. 4b) and then decreases. The CI at which the maximal diffuse PAR occurs appears to be larger than the CI at which the CO_2 uptake reaches its maximum (compare Fig. 4b with Fig. 3), which is different from what happens in a forest ecosystem (Gu et al., 1999). This is consistent with the fact that, in the semi-arid region, the vegetation reaches light saturation before the maximum diffuse PAR appears. The fraction of diffuse PAR typically ranges from about 0.1 to 1.0. When the CI is roughly less than 0.4, D_f is close to one (>0.9), which corresponds to the overcast sky conditions of optically thick clouds. But as CI increases, D_f decreases rapidly to values nearing 0.1. The results of Figs. 3 and 4 clearly show that the increase and decrease in the carbon uptake by the vegetation for the CI values lower and greater than around 0.4, respectively, are due primarily to the availability of diffuse radiation.

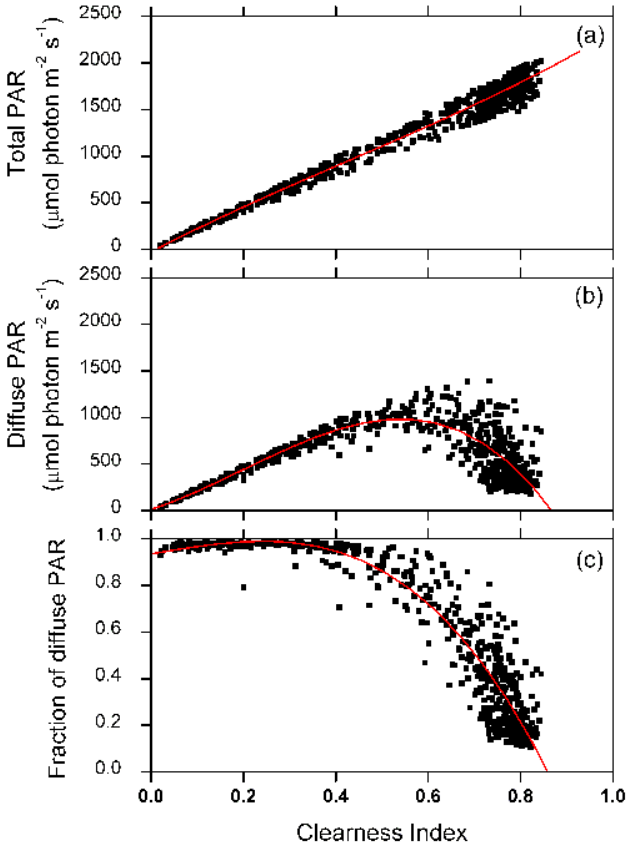

Fig. 4. Relationships between total PAR **(a)**, and diffuse PAR **(b)**, and the fraction of diffuse PAR **(c)**, and clearness index for 3rd polynomial fits ($n = 663$, (a) $r^2 = 0.98$, (b) $r^2 = 0.68$, (c) $r^2 = 0.92$, $p < 0.01$), respectively.

Indeed, observations during the growing season show clearly a significant increase in the daytime CO_2 exchange for large values of D_f (associated with CI values below light-saturation levels), and a decrease for low values of D_f (associated with CI values above the light-saturation point). The F_c values normalized by total PAR and plotted against D_f are shown in Fig. 5, clearly displaying the effect of D_f on carbon exchange. The light use efficiency of vegetation remains relatively constant with increase in D_f, dropping sharply after $D_f > 0.6$, indicating that for higher diffuse fraction, the light use efficiency for the grass vegetation enhances significantly as a result of increased D_f in the semi-arid Loess Plateau regions. Additionally, for the short-statured vegetation, due to the important effect of temperature on the respiration, we stratify the analyses by temperature. From Fig. 5b, we can see that the LUE increases with decreased air temperature caused by the presence of clouds, but the extent of increased LUE declines with the increased temperature corresponding to the decreased cloudiness. In addition, it is notable that for each temperature intervals, when the fraction of diffuse PAR is higher, the LUE of vegetation increases with the increased

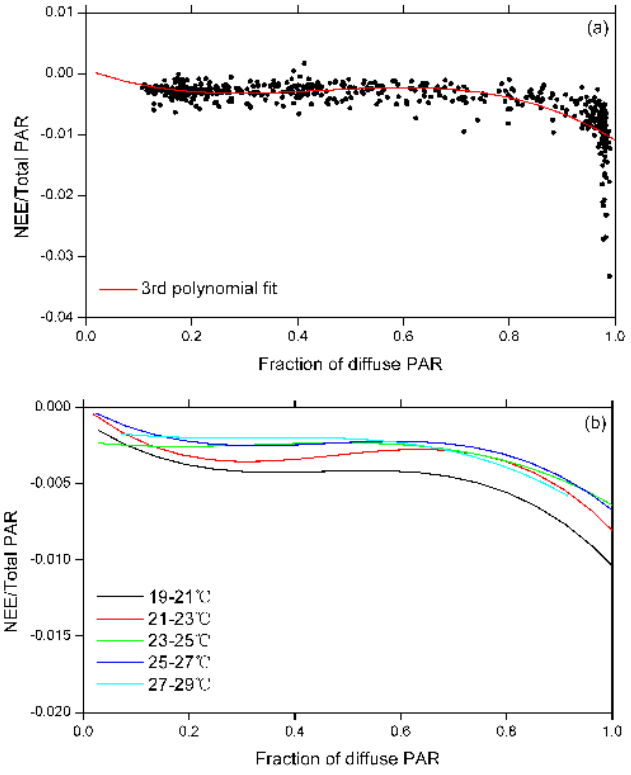

Fig. 5. Light use efficiency of vegetation as a function of the fraction of diffuse PAR for all the data **(a)** and the air temperature at 2 m of 19–21°, 21–23°, 23–25°, 25–27° and 27–29° intervals **(b)**. 3rd polynomial fits (a) $n = 540$, $r^2 = 0.55$, $p < 0.01$; (b) $n = 85$, $r^2 = 0.40$, $p < 0.01$; $n = 127$, $r^2 = 0.66$, $p < 0.01$; $n = 118$, $r^2 = 0.38$, $p < 0.01$; $n = 88$, $r^2 = 0.45$, $p < 0.01$; $n = 34$, $r^2 = 0.24$, $p < 0.01$ are shown.

D_f, indicating that the enhanced LUE is caused mainly by increased diffuse fraction rather than temperature, as same as Fig. 5a.

4.3 Effect of clouds

The diurnal variation in the diffuse fraction and its impact on CO_2 flux can be understood in terms of related changes in cloud cover and atmospheric aerosol loading. Clouds reduce the total solar radiation but increase the relative proportion of diffuse radiation at the Earth surface. Figure 6a and b show the fraction of diffuse PAR and CI as a function of cloudiness, respectively. The D_f increases almost linearly with cloudiness. The CI, on the other hand, remains relatively constant at around 0.8 as cloudiness increases to around 0.6, decreasing rapidly thereafter to around 0.4 as CI approaches 1. It is also noted that under an overcast condition the CI values change from 0.4 to 0. Thus, in reference to Figs. 4c, 6a and b, we can categorize the data into $D_f > 0.9$ and $D_f \leq 0.9$ regimes, with the former associated with the overcast sky condition of optically thick clouds. The two regimes correspond to the CI less than and larger than about 0.4, respectively (Fig. 4c).

For the very high D_f (>0.9), the NEE of CO_2 (absolute values) increases with the clearness index (i.e., net carbon uptake increase, a sink) (Fig. 7a), until the vegetation reaches its light saturation point. Several researchers have suggested that even though cloudiness results in larger values of D_f (relative increase in diffuse radiation), the total radiation is dramatically reduced, leading to lower, rather than higher carbon uptake in some ecosystems (Krakauer and Randerson, 2003). As indicated in Figs. 4c and 7, the carbon uptake decreases with decreasing CI (corresponding to the decreased Rg) for optically thick clouds. However, the frequency distribution histograms of S and CI for $D_f > 0.9$ (not shown) shows that the most frequent S values fall in the 300–500 Wm^{-2} category, and the CI is mainly less than 0.4, indicating that for $D_f > 0.9$, S is near the light saturation point. In fact, the results of Fig. 4a and c both show that for $D_f > 0.9$, S is basically less than about 500 $W\,m^{-2}$, which is near the light saturation values for short grass vegetation around our observation site. Thus, the overcast sky conditions of optically thick clouds will lead to higher NEE for a semi-arid grassy region, owing to the lower light saturation point and the higher light use efficiencies (see Fig. 5). It also shows that the short grass ecosystem can tolerate exceedingly large reductions in solar radiation without lowering its carbon uptake capacity.

Additionally, according to Fig. 3, the greatest carbon uptake is associated with CI between 0.3–0.5; the frequency distributions of D_f for that CI interval are given (Table 1). The result shows that most data are located in the 0.9–1.0 category, indicating that a maximum carbon uptake by the short-grass ecosystem at our site occurs under the overcast condition with optically thick clouds. In addition to the light saturation factor discussed above, the diffuse radiation under overcast conditions with optically thick clouds results in higher light use efficiencies by plant canopies. For the United States, Min (2005) showed that the radiation use efficiency of the CO_2 uptake process under optically thick clouds is higher than under aerosol and patchy/thin clouds. Our results provide additional evidence that the carbon uptake will increase with diffuse fraction under optically thick clouds, but for an entirely different ecosystem.

When the diffuse fraction is less than or equal to 0.9, CI is generally larger than 0.4, corresponding to the S larger than about 500 $W\,m^{-2}$ (see Fig. 4). The fraction of diffuse PAR increases as CI decreases from 0.85 to about 0.4 and the cloudiness increases (Fig. 6a and b). However, when the total solar radiation has reached or exceeded the light saturation level of the short-grass vegetation at our study site, the CO_2 uptake will be no longer increase, but could in fact decrease slightly with increasing CI (see Fig. 3). Since the optical properties of clouds do not depend only on the cloudiness, but also on other physical characteristics of the clouds, such as cloud shapes, thickness and size distribution, NEE of

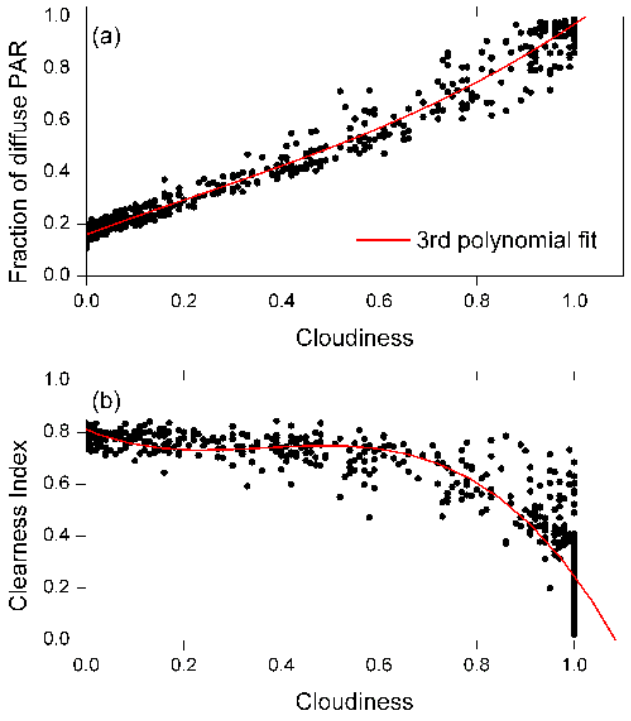

Fig. 6. Relationships between fraction of diffuse PAR **(a)**, clearness index **(b)** and cloudiness, respectively for 3rd polynomial fits ($n = 663$, (a) $r^2 = 0.98$, (b) $r^2 = 0.86$, $p < 0.01$).

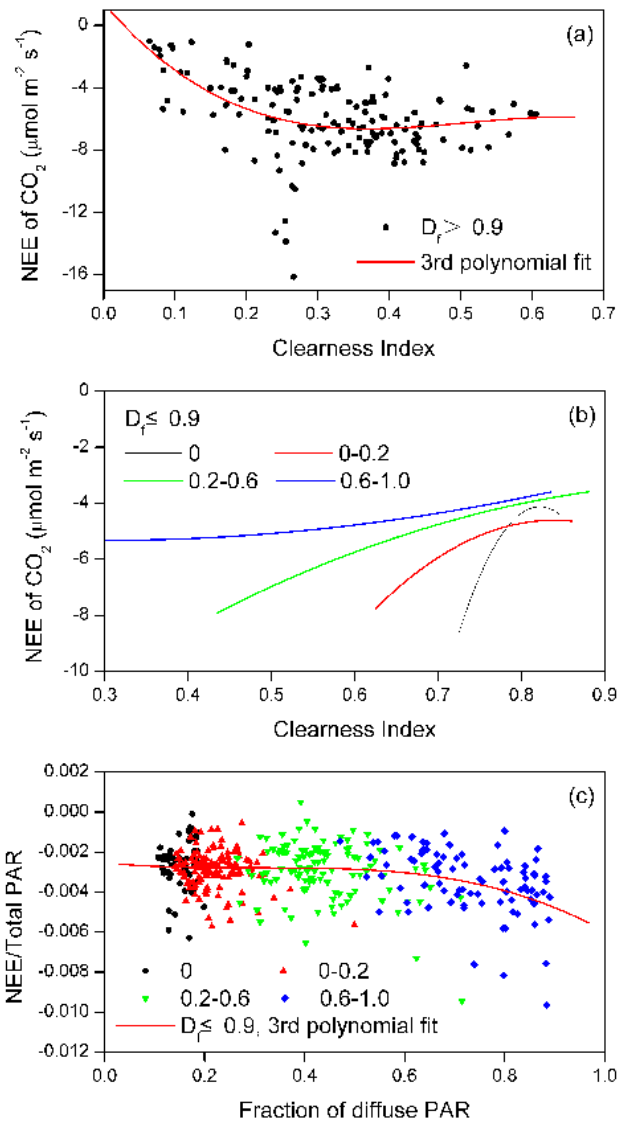

Fig. 7. Relationships between NEE of CO_2 and clearness index for $D_f > 0.9$ **(a)**, and for $D_f \leq 0.9$ **(b)**, and the light use efficiency of vegetation as a function of fraction of diffuse PAR for $D_f \leq 0.9$ **(c)** grouping the data according to the cloudiness of 0, 0–0.2, 0.2–0.6 and 0.6–1.0 intervals; (a) 3rd polynomial fit ($n = 150$, $r^2 = 0.23$, $p < 0.01$) is shown. (b) 2nd polynomial fits (0: $n = 58$, $r^2 = 0.15$, $p < 0.01$; 0–0.2: $n = 129$, $r^2 = 0.07$, $p < 0.01$; 0.2–0.6: $n = 115$, $r^2 = 0.07$, $p < 0.05$; 0.6–1.0: $n = 86$, $r^2 = 0.05$, $p < 0.05$) are shown, (c) 3rd polynomial fit ($n = 388$, $r^2 = 0.11$, $p < 0.01$) is shown for all the data.

CO_2 does not show a simple direct relationship with cloudiness (not shown). For $D_f \leq 0.9$, Fig. 7b shows a relationship between NEE and CI for different cloudiness intervals of 0, 0–0.2, 0.2–0.6, 0.6–1.0. The result shows that the carbon uptake decreases with increasing cloudiness for the same CI, and the CI decreases as the cloudiness increases. However, when we normalize NEE by the total PAR (Fig. 7c), we see that, when $D_f \leq 0.9$, the fraction of diffuse radiation and light use efficiency of the vegetation are both enhanced with increasing cloudiness (especially when it is larger than 0.6). This result is consistent with the effect of diffuse radiation, as expressed by the clear relationship between D_f and the cloudiness (see Fig. 6a).

The above explanations about the observed changes in the carbon uptake with the cloudiness focus only on the effects of diffuse radiation. However, the presence of clouds is a result of changes in many atmospheric factors such as air and soil temperature, VPD, precipitation, etc. These factors all have direct or indirect influences on the short grass ecosystems and the overlying atmosphere. Indeed, the boundary layer meteorological observation at the SACOL site shows that changes in multiple environmental factors which can influence canopy photosynthesis and/or ecosystem respiration exist as the cloudiness varies.

Figure 8 shows the diurnal cycles (07:00–19:00) of air temperature, soil temperature, and vapor pressure deficit (VPD) under three kinds of sky conditions (i.e., clear (non-cloudy), cloudy ($0.6 <$ cloudiness < 1) and overcast (cloudiness $= 1$)). Carbon uptake can be enhanced by decreases in leaf and soil respirations. In general, temperature is one of the major controlling factors in both the leaf and

Table 1. Frequency distribution of the fraction of diffuse PAR (D_f) for 0.3<CI<0.5.

0.3<CI<0.5	The fraction of diffuse PAR (D_f)		
	0.7–0.8	0.8–0.9	0.9–1.0
Frequency (%)	4.2	10.4	85.4

soil respirations. Figure 8a and b show that air and soil temperatures tend to decrease under cloudy and overcast conditions, especially under overcast conditions. This is because of reduced radiative forcing under cloudy and overcast conditions. The decreases in temperature reduce leaf and soil respiration and thus contribute to the enhancement of ecosystem carbon uptake under cloudy and overcast conditions. The general decreasing trends in VPD under cloudy and overcast conditions (Fig. 8c) induce stomatal openness and thus enhance leaf photosynthesis (Freedman et al., 1998; Collatz et al., 1991).

In addition, according to Fig. 5b, under overcast and cloudy sky conditions with reduced air temperature, the light use efficiency of vegetation is enhanced. However, a further analysis is required to determine if, under cloudy condition, the increased carbon uptake is caused by the decrease in respiration (due to temperature decrease) or by enhanced photosynthesis. From Fig. 8a, we see that under overcast conditions when the solar elevation angle is larger than 50°, the average air temperature is between 16 and 19°, nearly corresponding to the temperature of maximum photosynthesis (Fig. 9b) and reduced ecosystem respiration (Fig. 9c), thus resulting in a maximum carbon uptake. Furthermore, the result of the fitted curve (using Eq. 5) to the observed data (Fig. 9c) shows that, as the air temperature increases from 12 to 30 °C, the ecosystem respiration rate increases only from around 1.17 to 1.30 $\mu mol\, m^{-2}\, s^{-1}$, while the canopy photosynthesis shows a significant reduction from around 7.71 to 3.15 $\mu mol\, m^{-2}\, s^{-1}$. Therefore, the CO_2 uptake decreases with the increased temperature (Fig. 9a). The temperature at which maximum carbon uptake occurs at the SACOL site with grassland is much less than that with cropland (Norman et al., 1991). These relationships also confirm the fact that the vegetation canopy at SACOL reaches the light saturation point at a lower temperature, resulting in a carbon uptake reduction with higher temperatures. Considering all these factors, we can conclusively state that the light use efficiency of a short grass-covered site is enhanced as a result of an increased diffuse fraction of radiation (Figs. 5 and 7c).

4.4 Effect of aerosol loading

It is well known that scattering by aerosols also increases the diffuse fraction of incident radiation. In order to delineate the effect of aerosol loading only (without clouds) on diffuse

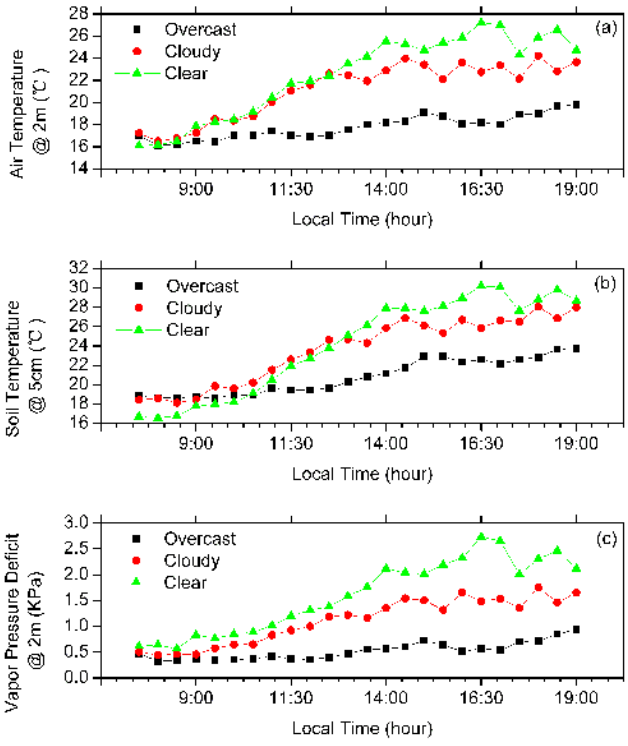

Fig. 8. Comparison of averaged air temperature, soil temperature and vapor pressure deficit under three sky conditions (i.e., clear (non-cloudy), cloudy (0.6<cloudiness<1) and overcast (cloudiness=1)) from 07:00 to 19:00 LT.

fraction, we use clear-sky data to analyze for AOD (aerosol optical depth). At the SACOL site, simultaneous measurements of F_e and AOD are available for July–August of 2007. AOD data related to 500 nm are chosen since they correspond to a photosynthetically active radiation (PAR) wavelength (400–700 nm). Figure 10 shows a near linear relation between D_f and aerosol loading, indicating that a larger aerosol loading results in an increase of the fraction of diffuse PAR. However, rarely does D_f become greater than around 0.6, allowing total solar radiation to surpass the grassland light saturation point quickly.

In Fig. 11, the correlation is not strong, but for the narrow range of CI (CI of 0.7 to 0.8), the high aerosol loadings appear to result in lower values for photosynthesis. We also note that even under a high aerosol loading condition, CI can still be large, corresponding to a high solar radiation (about 900 $W\, m^{-2}$). The results from Figs. 10 and 11 show that the presence of aerosols leads to an increase in diffuse PAR fraction. However, unlike the situation under overcast conditions of optically thickness cloud, aerosol loading has a negligible impact on respiration, but reduces the photosynthesis, and may result in decreasing CO_2 uptake by the semi-arid ecosystem at the SACOL site. It is similar with the changes of NEE as the cloudiness increase when $D_f \leq 0.9$, and the solar radiation also exceeds the light saturation of short-grass

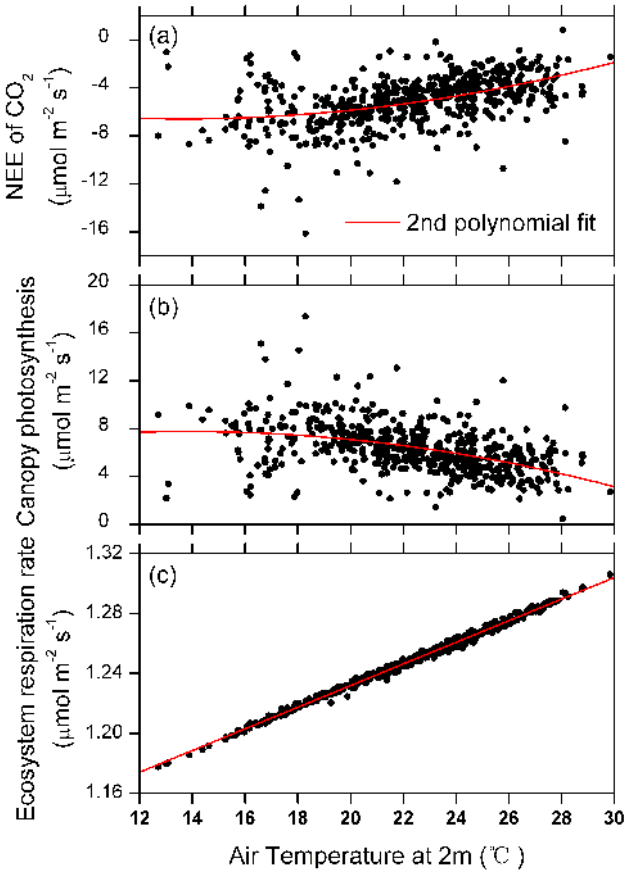

Fig. 9. Relationships between NEE of CO_2 **(a)**, canopy photosynthesis **(b)**, ecosystem respiration rate **(c)**, and air temperature for 2nd polynomial fits ($n = 540$, (a) $r^2 = 0.22$, (b) $r^2 = 0.22$, (c) $r^2 = 0.99$, $p < 0.01$).

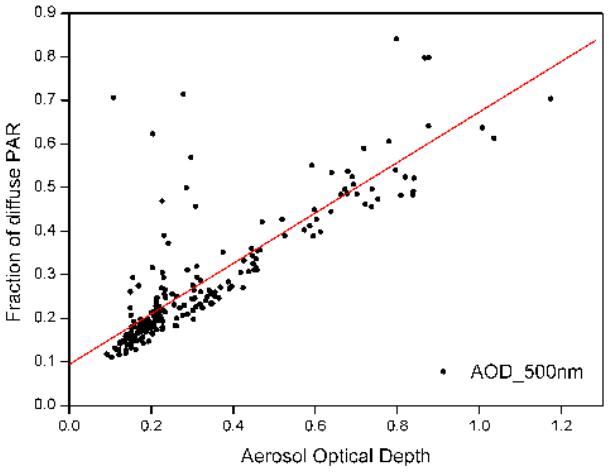

Fig. 10. Relationship between Aerosol optical depth (AOD) and fraction of diffuse PAR (D_f) for linear fit ($n = 209$, $r^2 = 0.69$, $p < 0.01$).

vegetation. In addition, since the D_f values are mostly less than 0.6, according to Fig. 5, the light use efficiency of the vegetation remains relatively constant with increasing AOD (not shown). Although there is a significant amount of scatter, the results show a tendency of decreasing carbon uptake with increasing AOD for all AOD wavelengths (not shown).

In addition, under a clear sky condition the air temperature is higher than that under other sky conditions (Fig. 8). From Fig. 9, we see the CO_2 uptake reduces with the increased air temperature. Thus, a further analysis is required to see if the effect of aerosol loading on the carbon uptake is also significant under same temperature. Indeed, a relationship between CI and air temperature under low and high aerosol loading indicates that the temperature is lower for higher AOD than that for lower AOD (not shown) at the same CI. Figure 12 suggests that the carbon uptake decreases slightly with the increased AOD for the same temperature. However, the weakening extent of carbon uptake with AOD is decreased compared with that in Fig. 11. Although this seems to indicate the existence of a negative effect of AOD on carbon uptake, it may not be a major factor in regulating the ecosystem carbon exchange.

Previous studies on the effect of aerosol loading on CO_2 uptake have suggested that aerosols exert a positive function on the terrestrial carbon cycle, at least for forest and cropland ecosystems (e.g., Gu at al., 2003; Niyogi et al., 2004). Our different results for a semi-arid grassland ecosystem show the importance of canopy structure of an ecosystem and its photosynthetic interaction with the radiation field. Niyogi et al. (2004) did analyze the effects of aerosol loading on NEE over different ecosystem landscapes, and the results for the grasslands also show a negative response to the aerosols, which is consistent with our results.

5 Conclusions

This paper has reported results of the sensitivity of NEE of CO_2 to changes in the nature of radiative forcing caused by variations in clouds and aerosol loading over a semi-arid grass ecosystem at Loess Plateau in northwest China. We have made use of the observational data taken at the SACOL site during the midgrowing (July–August) season of 2007. For our site we have found that the light use efficiency of vegetation under cloudy and overcast conditions is significantly enhanced by a large fraction of diffuse PAR (>0.6), and the CO_2 uptake during the midgrowing season reaches a maximum under overcast conditions of optically thick clouds, though the total solar radiation itself decreases significantly. However, an increase in D_f caused by the increased cloudiness (except for the overcast conditions) actually reduces the carbon uptake. The aerosol loading also shows a slight tendency to decrease the carbon uptake.

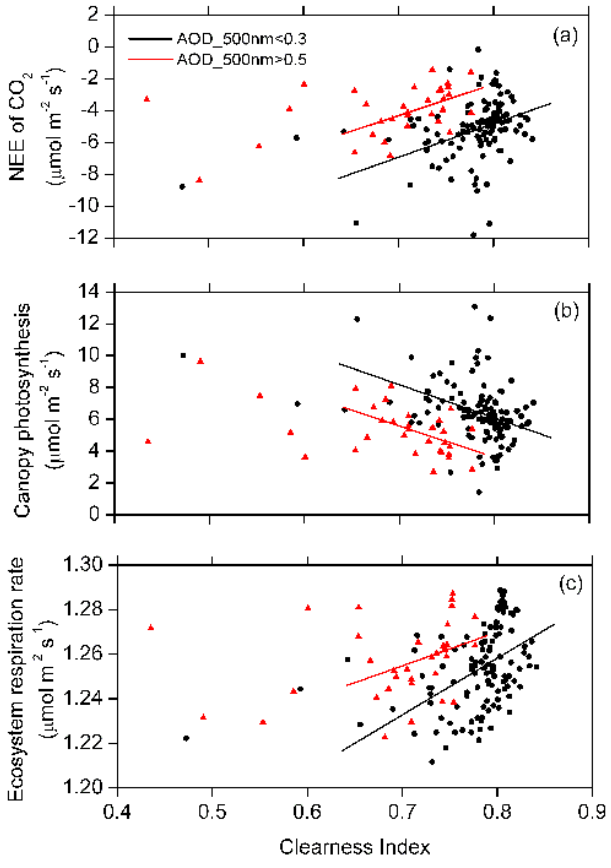

Fig. 11. Relationships between NEE of CO_2 **(a)**, canopy photosynthesis **(b)**, ecosystem respiration rate **(c)**, and clearness index for linear fits. For CI>0.65, black line: AOD<0.3 ($n = 115$, (a) $r^2 = 0.13$, (b) $r^2 = 0.13$, (c) $r^2 = 0.20$, $p < 0.01$); red line: AOD>0.5 ($n = 28$, (a) $r^2 = 0.25$, $p < 0.01$, (b) $r^2 = 0.25$, $p < 0.01$, (c) $r^2 = 0.11$, not passing the significance test).

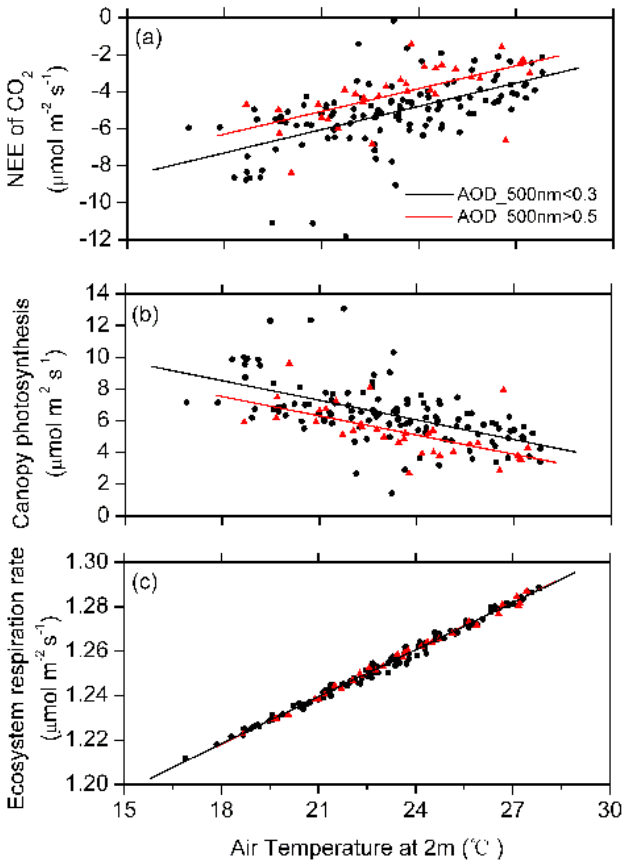

Fig. 12. Relationships between NEE of CO_2 **(a)**, canopy photosynthesis **(b)**, ecosystem respiration rate **(c)**, and air temperature for linear fits. Black line: AOD<0.3 ($n = 118$, (a) $r^2 = 0.33$, (b) $r^2 = 0.32$, (c) $r^2 = 0.99$, $p < 0.01$); red line: AOD>0.5 ($n = 33$, (a) $r^2 = 0.40$, (b) $r^2 = 0.39$, (c) $r^2 = 0.99$, $p < 0.01$).

The CO_2 uptake increases with CI until the light saturation point of the grass (CI≈0.37) is reached. Thereafter, carbon uptake decreases with increasing CI. The relationship between D_f and CI shows that the fraction of diffuse PAR remains relatively constant near 0.9–1.0 for CI up to around 0.4, but decreases rapidly with increasing CI thereafter. For the semi-arid grassland at our site, a maximum carbon uptake occurs under overcast conditions of optically thick clouds ($D_f > 0.9$). For $D_f \leq 0.9$, the CO_2 uptake decreases as cloudiness increases, but the light use efficiency is enhanced due to the occurrence of larger fraction of diffuse PAR under greater cloudiness. Furthermore, compared with the direct radiation under clear sky condition, it takes longer for diffuse radiation to reach the light saturation point, further enhancing the uptake of CO_2 by the vegetation under cloudy sky conditions. In addition, under cloudy conditions, many environmental factors can affect the carbon uptake, e.g., decreases in air temperature, soil temperature, and vapor pressure deficit, by either promoting canopy photosynthesis or reducing leaf and soil respiration. For a short grassland with smaller LAI (about 0.37), respiration is less sensitive than photosynthesis to temperature change; that is, the rate of ecosystem respiration increase is less than the rate of photosynthetic decrease for a given temperature increase. Thus, the maximum CO_2 uptake occurs under overcast sky condition of optically thick cloud with lower temperature. However, the light use efficiencies of vegetation are enhanced with the greater fraction of diffuse radiation for the same temperature intervals.

In contrast to the "positive" effect of overcast conditions, the fraction of diffuse PAR increases with the aerosol loading (as measured by AOD) under clear sky conditions, but only to values of about 0.6, when the solar radiation surpasses the photosynthetic light saturation point of the grassland quickly, thereby decreasing the CO_2 uptake (by decreased photosynthesis) with increasing CI. Under clear sky conditions, increase in AOD may result in decreasing net CO_2 exchange due to the increased fraction of diffuse PAR, which is also enhanced as the wavelengths of AOD increase.

The effect of clouds and aerosols on a semi-arid grassland ecosystem CO_2 exchange is still poorly understood, especially for aerosols. Clouds and aerosols can alter irradiance at the top of the atmosphere and even more profoundly at the surface and affect the biosphere (Schwartz, 1996). Changes in diffuse fraction, due to clouds and aerosol loading, can have potential impact on the terrestrial carbon exchange. At the SACOL site characterized by a short grassland ecosystem with smaller LAI values (about 0.37), the impact of diffuse radiation has been elucidated in this paper. We have found that the photosynthetic enhancement due to diffuse radiation is not as large as has been observed at forest and cropland ecosystems, due to the fact that most of the grass leaves are exposed to the direct solar radiation, as well as to the fact that a grassland ecosystem has lower light saturation point than either forest or cropland. It is notable that after the canopy of vegetation has reached the light saturation at SACOL site, the greater fraction of diffuse PAR caused by clouds and aerosols result in the decreased CO_2 uptake. It may be due to the canopy architecture and need the further analysis in our future work. Furthermore, the influence of other environment factors may be more important than the diffuse radiation for a vegetation with smaller LAI.

This paper is a preliminary study of clouds and aerosol loading effects on the carbon uptake by a grass ecosystem located at the semi-arid Loess Plateau region. We have introduced evidence to show that an overcast sky with optically thick clouds can cause a maximum CO_2 uptake, even though the direct solar radiation is significantly reduced. The light use efficiency of vegetation is significantly enhanced under cloudy conditions with higher fraction of diffuse PAR. We have also shown that a routine aerosol loading from natural or anthropogenic sources can also have a certain influence on a semi-arid regional NEE of CO_2, without significantly reducing the total radiation itself. Thus, both the cloudiness condition and the aerosol loading have been shown in this study to have a major forcing on the NEE of CO_2 of the semi-arid grassland ecosystem at our study site.

In order to obtain a more robust result regarding interannual variability of the CO_2 flux at the SACOL site, and its response to the interannual variation of clouds and aerosols, we need to analyze a longer dataset covering at least several years. This study is now underway.

Appendix A

Estimating cloudiness

The absorption, reflection and scattering effects of clouds influence the amount of solar radiation reaching the surface. An analysis of the effect of clouds on solar radiation can lead to obtaining a relationship between the downward shortwave radiation (SW) and cloudiness. In order to characterize the effect of clouds, we introduce the downwelling diffuse cloud effect, as the difference between the measured and clear-sky diffuse shortwave radiation. The clear-sky shortwave radiation estimation results are used to calculate the normalized downwelling diffuse cloud effect (D_n), where the diffuse cloud effect is normalized (divided) by the clear-sky total shortwave radiation (SW) to help remove the solar zenith angle dependence:

$$D_n = \frac{SW^{diffuse}_{measure} - SW^{diffuse}_{clear}}{SW^{total}_{clear}} \quad (A1)$$

Thus, the estimation of clear-sky shortwave radiation is the first condition that should be solved. Long et al. (2000) develop an algorithm to identify the clear sky using the surface shortwave radiation. This makes it easier to calculate the clear-sky diffuse radiation and total shortwave radiation at any time under cloudy conditions. Finally, we get the normalized downwelling diffuse cloud effect (D_n) using Eq. (A1).

To estimate the cloudiness using D_n, it is necessary to get the relationship between D_n and cloudiness on a one to one basis. In order to separate the overcast time with thicker optical depth from the partly cloud time and overcast time with thinner optical depth, we introduce a ratio, which is the measured total shortwave radiation divided by the clear-sky total shortwave radiation ($SW^{total}_{measure}/SW^{total}_{clear}$). Under clear sky conditions the ratio is nearly 1.0, but much less than 1.0 under cloudy conditions. Thus, we use a value of 0.4 to differentiate the two cases. That is, if the ratio is less than 0.4, as clear sky, the cloudiness is 0; if more than 0.4, as overcast day, the cloudiness is 1.0.

For other cases, we generally use the magnitude and variability of the measured D_n and diffuse ratio (the ratio of diffuse shortwave radiation and total shortwave radiation, $SW^{diffuse}_{measure}/SW^{total}_{measure}$) to identify the significantly thick cloud sky. We consider the averaged diffuse ratio under overcast conditions to be larger than 0.9. In addition, for the overcast condition we set an additional constraint, i.e. $D_n < 0.37$ and the corresponding standard deviation of diffuse ratio is less than 0.05, which is suitable for distinguishing the overcast and cloudy sky conditions and eliminate the inherent system noise. In summary, for the results presented here, any data sample with D_n less than 0.37, whose corresponding average diffuse ratio is larger than 0.9 and whose diffuse ratio standard deviation is less than 0.05, is declared as overcast. The cloudiness is marked as 1.0.

We have assigned the cloudiness value of 0 and 1.0, respectively, for clear and overcast skies. For other conditions, we use the following exponential regression equation to get the cloudiness:

$$\text{Cloudiness} = 2.255(D_n)^{0.9381} \quad (A2)$$

The cloudiness calculated by Eq. (A2) shows a good consistency with the measured cloudiness. More details relating to the estimating fractional sky cover using D_n can be found in Long et al. (2006) and Wang (2009).

Acknowledgements. SACOL was sponsored by Lanzhou University through 985 Program; the National Science Foundation of China under Grant No. 40725015 and 40633017 and the National Basic Research Program of China under Grant No.2006CB400501. We are grateful for the excellent support provided by the people at the College of Atmospheric Sciences, Lanzhou University.

Edited by: J. G. Murphy

References

Abakumova, G. M., Feigelson, E. M., Russak, V., and Stadnik, V. V.: Evaluation of long-term changes in radiation, cloudiness, and surface temperature on the territory of the former Soviet Union, J. Climate, 9, 1319–1327, 1996.

Baldocchi, D. D., Hicks, B. B., and Meyers, T. P.: Measuring biosphere-atmosphere exchanges of biologically related gases with micrometeorological methods, Ecology, 69, 1331–1340, 1988.

Burba, G. G., McDermitt, D. K., Grelle, A., Anderson, D. J., and Xu, L.: Addressing the influence of instrument surface heat exchange on the measurements of CO_2 flux from open-path gas analyzers, Glob. Change Biol., 14, 1854–1876, doi:10.1111/j.1365-2486.2008.01606.x, 2008.

Chen, Y. H., Huang, J. P., Chen, C. H., Zhang, Q., Feng, J. D., Jin, H. C., and Wang, T. H.: Temporal and spatial distribution of cloud water resources over Northwestern China, Plateau Meteorology, 24(6), 905–912, 2005.

Chinese Soil Taxonomy Cooperative Research Group, Institute of Soil Science, Academic Sinica, Chinese Soil Taxonomy (revised proposal), Chinese Agricultural Sci-Tech Press, 218 pp., 1995 (in Chinese).

Collatz, G. J., Ball, J. T., Grivet, C., and Berry, J. A.: Physiological and environmental regulation of stomata conductance, photosynthesis and transpiration: A model that includes a laminar boundary layer, Agr. Forest Meteorol., 54, 107–136, 1991.

Fitzjarrald, D. R., Moore, K. E., Sakai, R. K., and Freedman, J. M.: Assessing the impact of cloud cover on carbon uptake in the northern boreal forest, in: Proceedings of the AGU Meeting, Spring 1995, H32E-5, S215, 1995.

Freedman, J. M., Fitzjarrald, D. R., Moore, K. E., and Sakai, R. K.: Boundary layer cloud climatology and enhanced forest-atmosphere exchange. 23rd Conference on Agricultural and Forest Meteorology, American Meteorological Society, Albequerque, NM, 1998.

Freedman, J. M., Fitzjarrald, D. R., Moore, K. E., and Sakai, R. K.: Boundary layer clouds and vegetation-atmosphere feedbacks, J. Climate, 14, 180–197, 2001.

Gao, Z., Lenschow, D. H., He, Z., and Zhou, M.: Seasonal and diurnal variations in moisture, heat and CO_2 fluxes over a typical steppe prairie in Inner Mongolia, China, Hydrol. Earth Syst. Sci., 13, 987–998, doi:10.5194/hess-13-987-2009, 2009.

Goudriaan, J.: Crop Micrometeorology: A Simulation Study. Center for Agricultural Publication and Documentation, Wageningen, 1977.

Gu, L., Fuentes, J. D., Shugart, H. H., Staebler, R. M., and Black, T. A.: Responses of net ecosystem exchanges of carbon dioxide to changes in cloudiness: Results from two North American deciduous forests, J. Geophys. Res., 104, 31421–31434, 1999.

Gu, L., Baldocchi, D., Verma, S. B., Black, T. A., Timo, V., Falge, E. M., and Dowty, P. D.: Advantages of diffuse radiation for terrestrial ecosystem productivity, J. Geophys. Res., 107(D6), 4050, doi:10.1029/2001JD001242, 2002.

Gu, L., Baldocchi, D. D., Wofsy, S. C., Munger, J., Michalsky, J., Urbanski, S. P., and Boden, T. A.: Response of a deciduous forest to the Mount Pinatubo eruption: Enhanced photosynthesis, Science, 299, 2035–2038, 2003.

Holben, B. N., Eck, T. F., Slutsker, I., Tanre, D., Buis, J. P., Setzer, A., Vermote, E., Reagan, J. A., Kaufman, Y. J., Nakajima, T., Lavenu, F., Jankowiak, I., and Smirnov, A.: AERONET—A federated instrument network and data archive for aerosol characterization, Remote Sens. Environ., 66, 1–16, 1998.

Holben, B. N., Tanre, D., Smirnov, A., Eck, T. F., Slutsker, I., Abuhassan, N., Newcomb, W. W., Schafer, J. S., Chatenet, B., Lavenu, F., Kaufman, Y. J., Castle, J., Setzer, A., Markham, B., Clark, D., Frouin, R., Halthore, R., Karneli, A., O'Neill, N., Pietras, C. Pinker, R., Voss, K., and Zibordi, G.: An emerging ground-based aerosol climatology: Aerosol optical depth form AERONET, J. Geophys. Res., 106, 12067–12097, 2001.

Hollinger, D. Y., Kelliher, F. M., Byers, J. N., Hunt, J. E., McSeveny, T. M., and Weir, P. L.: Carbon dioxide exchange between an undisturbed old-growth temperate forest and the atmosphere, Ecology, 75, 134–150, 1994.

Huang, J. P., Zhang, W., Zuo, J., Bi, J., Shi, J., Wang, X., Chang, Z., Huang, Z., Yang, S., Zhang, B., Wang, G., Feng, G., Yuan, J., Zhang, L., Zuo, H., Wang, S., Fu, C., and Chou, J.: An overview of the semi-arid climate and environment research observatory over the Loess Plateau, Adv. Atmos. Sci., 25(6), 906–921, doi:10.1007/s00376-008-0906-7, 2008.

Jarvis, P. G. and Leverenz, J. W.: Productivity of temperate, deciduous and evergreen forests, in: Physiological Plant Ecology IV, (Encyclopedia of Plant Physiology, NS, vol 12D), edited by: Lange, O. L., Nobel, P. S, Osmond, C. B., and Ziegler, H., Springer, Berlin Heidelberg New York, 233–280, 1983.

Ji, G. L., Ma, X. Y, Zou, J. L., and Lv, L. Z.: Characteristics of the photosynthetically active radiation over Zhangye region, Plateau Meteorology, 12(2), 141–146, 1993 (in Chinese).

Krakauer, N. Y. and Randerson, J. T.: Do volcanic eruptions enhance or diminish net primary production? Evidence from tree rings, Global Biogeochem. Cy., 17(4), 1118, doi:10.1029/2003GB002076, 2003.

Letts, M. G., Lafleur, P. M., and Roulet, T.: On the relationship between cloudiness and net ecosystem carbon dioxide exchange in a peatland ecosystem, Ecoscience, 12, 53–59, 2005.

Liu, H. Z., Tu, G., Dong, W. J., Fu, C. B., and Shi, L. Q.: Seasonal and diurnal variations of the exchange of water vapor and CO_2 between the land surface and atmosphere in the semi-arid area, Chinese, J. Atmos. Sci., 30(1), 108–117, 2006 (in Chinese).

Liu, X. D., Bai, H., Ning, H., Guo, J., and Dong, A.: Response of arid meteorological disaster to climatic warming in Gansu Province, J. Glaciol. Geocryol., 28(5), 707–712, 2006 (in Chinese).

Long, C. N. and Ackerman, T. P.: Identification of clear skies from broadband pyranometer measurements and calculation of downwelling shortwave cloud effects, J. Geophys. Res., 105(D12), 15609–15626, 2000.

Long C. N., Ackerman, T. P., Gaustad, K. L., and Cole, J. N. S.: Estimation of fractional sky cover from broadband short-

wave radiometer measurements, J. Geophys. Res., 111, D11204, doi:10.1029/2005JD006475, 2006.

Mercado, L., Bellouin, N., Sitch, S., Boucher, O., Huntingford, C., Wild, M., and Cox, P. M.: Impact of changes in diffuse radiation on the global land carbon sink, Nature, 458, 1014–1017, 2009.

Michalsky, J.: The Astronomical Almanac's algorithm for approximate solar position (1950–2050), Sol. Energy, 40(3), 227–235, 1988.

Min, Q.: Impacts of aerosols and clouds on forest-atmosphere carbon exchange, J. Geophys. Res., 110, D06203, doi:10.1029/2004JD004858, 2005.

Niyogi, D., Chang, H., Saxena, V. K., Holt, T., Alapaty, K., Booker, F., Chen, F., Davis, K., Holben, B., Matsui, T., Meyers, T., Oechel, W., Pielke Sr., Wells, R., Wilson, K., and Xue, Y. K.: Direct observations of the effects of aerosol loading on net ecosystem CO_2 exchanges over different landscapes, Geophys. Res. Lett., 31, L20506, doi:10.1029/2004GL020915, 2004.

Norman, J. M. and Arkebauer, T. J.: Predicting canopy light-use efficiency from leaf characteristics, in: Modeling Plant and Soil Systems, edited by: Hanks, J. and Ritchie, J., Agronomy Monograph, ASA-CSSA-SSSA, 125–143, 1991.

Oliphant, A. J., Schmid, H. P., Grimmond, C. S. B., Su, A.-B., Scott, S., and Vogel, C.: The role of cloud cover in net ecosystem exchange of CO_2 over two mid-western mixed hardwood forests, Abstracts of 25th Conference on Agricultural and Forest Meteorology, American Meteorological Society, Norfolk, Virginia, 2002.

Oliveira, P. H. F., Artaxo, P., Pires, C., Lucca, S. D., Procopio, A., Holben, B., Schafer, J., Cardoso, L. F., Wofsy, S. C., and Rocha, H. R.: The effects of biomass burning aerosols and clouds on CO_2 flux in Amazonia, Tellus B, 59, 338–349, 2007.

Price, D. T. and Black, T. A.: Effects of short-term variation in weather on diurnal canopy CO_2 flux and evapotranspiration of a juvenile Douglas-Fir stand, Agr. Forest Meteorol., 50, 139–158, 1990.

Roderick, M. L., Farquhar, G. D., Berry, S. L., and Noble, I. R.: On the direct effect of clouds and atmospheric particles on the productivity and structure of vegetation, Oecologia, 129, 21–30, 2001.

Schwartz, S. E.: The Whitehouse Effect – Shortwave radiative forcing of climate by anthropogenic aerosols: an overview, J. Atmos. Sci., 27, 359–382, 1996.

Song, L. C. and Zhang, C. J: Changing features of precipitation over Northwest China during the 20th century, J. Glaciol. Geocryol., 25(2), 143–148, 2003 (in Chinese).

Spitters, C. J. T., Tussaint, H. A. J. M., and Goudriaan, J.: Separating the diffuse and direct component of global radiation and its implications for modeling canopy photosynthesis, Part I, Components of incoming radiation, Agr. Forest Meteorol., 38, 217–229, 1986.

Suraqui, S., Tabor, H., Klein, W. H., and Goldberg, B.: Solar radiation changes at Mt. St. Katherine after forty years, Sol. Energy, 16, 155–158, 1974.

Wang, T. H.: Retrieving optical and microphysical properties of mixed-phase and dusty cloud over Northwestern China from MFRSR, Ph. D. dissertation, Lanzhou Univ., Lanzhou, China, 90–92, 2009 (in Chinese).

Yao, Y. B., Li, Y. B., Zhang, M. C., Wang, W. T., and Zhang, X. Y.: Response on climate in Longdong loess plateau to globe warming and fruit development impacted, Journal of Nanjing Forestry University (Natural Sciences Edition), 29(4), 73–77, 2005a (in Chinese).

Yao, Y. B., Wang, Y. R., Li, Y. H., and Zhang, X. Y.: Climate warming and drying and its environmental effects in the Loess Plateau [J], Resour. Sci., 27(5), 146–152, 2005b (in Chinese).

Zhou, Y. H., Xiang, Y. Q., and Luan, L. K.: Climatological estimation of quantum flux densities. Acta Meteorol. Sin., 54(4), 447–455, 1996 (in Chinese).

Zuo, J., Huang, J., Wang, J. M., et al: Surface turbulent flux measurements over the Loess Plateau for a semi-arid climate change study, Adv. Atmos. Sci., 26(4), 679–691, doi:10.1007/s00376-009-8188-2, 2009.